

Single-species dinoflagellate cyst carbon isotope ecology across the Paleocene-Eocene Thermal Maximum

Appy Sluijs¹, Linda van Roij¹, Joost Frieling¹, Jelmer Laks¹, and Gert-Jan Reichart^{1,2}

¹Department of Earth Sciences, Faculty of Geosciences, Utrecht University, Heidelberglaan 2, 3584CS Utrecht, Netherlands

²NIOZ (Royal Netherlands Institute for Sea Research), Department of Ocean Systems, and Utrecht University, PO Box 59, 1790AB Den Burg, Netherlands

ABSTRACT

We present the first ever species-specific fossil dinoflagellate cyst stable carbon isotope ($\delta^{13}\text{C}$) records, from the Bass River Paleocene-Eocene Thermal Maximum (PETM) section in New Jersey (USA), established using a novel coupled laser ablation–isotope ratio mass spectrometer setup. Correspondence with carbonate $\delta^{13}\text{C}$ records across the characteristic negative carbon isotope excursion indicates that the $\delta^{13}\text{C}$ of dissolved inorganic carbon exerts a major control on dinocyst $\delta^{13}\text{C}$. Pronounced and consistent differences between species, however, reflect different habitats or life cycle processes and different response to $p\text{CO}_2$. Decreased interspecimen variability during the PETM in a species that also drops in abundance suggests a more limited niche, either in time (seasonal) or space. This opens a new approach for ecological and evolutionary reconstructions based on organic microfossils.

INTRODUCTION

Fossilizable organic cyst-producing dinoflagellates are ecologically diverse unicellular eukaryotes, and include freshwater and marine, heterotrophic, mixotrophic, autotrophic, and polar and tropical species (Matthiessen et al., 2005). Dinoflagellate cyst (dinocyst) assemblages are widely used for paleoceanographic reconstructions of Triassic to modern seas and oceans, particularly along continental margins (Sluijs et al., 2005).

We explore the stable carbon isotopic composition ($\delta^{13}\text{C}$) of fossil dinocysts as a paleoceanographic indicator. Dinocyst $\delta^{13}\text{C}$ likely reflects the $\delta^{13}\text{C}$ of dissolved inorganic carbon ($\delta^{13}\text{C}_{\text{DIC}}$) (Sluijs et al., 2007). Culturing experiments have shown that dinoflagellate ^{13}C fractionation increases with seawater CO_2 concentrations, indicating potential for a CO_2 proxy (Hoins et al., 2016b, 2015; Van de Waal et al., 2013). Because cysts directly derive from dinoflagellates, $\delta^{13}\text{C}_{\text{DIC}}$ and seawater CO_2 concentrations are expected to affect dinocyst $\delta^{13}\text{C}$. A recently developed analytical setup allows for the analysis of tens of nanograms of particulate organic matter for $\delta^{13}\text{C}$ (Van Roij et al., 2017). This setup, laser ablation–nano combustion–gas chromatography–isotope ratio mass spectrometry (LA-nC-GC-IRMS) has been shown to achieve precise and accurate $\delta^{13}\text{C}$ values for higher plant pollen (Van Roij et al., 2017).

Over the first millennia of the Paleocene-Eocene Thermal Maximum (PETM, ca. 56 Ma), global surface temperatures warmed by $\sim 5^\circ\text{C}$ (Dunkley Jones et al., 2013; Frieling et al., 2017). This warming roughly coincided with deep ocean carbonate dissolution and a negative stable carbon isotope excursion (CIE) of several per mill recorded globally in sedimentary components, implying massive ^{13}C -depleted carbon injection into the ocean-atmosphere system (Dickens et al., 1997; Zachos et al., 2005).

The magnitude and structure of the CIE differ between bulk carbonate, species- and/or genus-specific foraminifera, bulk organic matter, and bulk dinocyst records at the Ocean Drilling Program Leg 174AX core at Bass River, New Jersey, USA (Cramer et al., 1999; John et al., 2008;

Sluijs et al., 2007) (Fig. DR1 in the GSA Data Repository¹). Moreover, pronounced regional biogeochemical and paleoenvironmental change has been recorded during the PETM (e.g., Gibbs et al., 2012; Kopp et al., 2009). The Bass River PETM section therefore presents a suitable case to (1) test the dependence of dinocyst $\delta^{13}\text{C}$ to large changes in both $\delta^{13}\text{C}_{\text{DIC}}$ and seawater carbonate chemistry, (2) evaluate whether this dependence is species specific, and (3) assess if dinocyst $\delta^{13}\text{C}$ values reflect changes in population ecology and/or biosynthesis. To this end, we analyzed the $\delta^{13}\text{C}$ of 4 dinocyst species with different ecological preferences across the CIE.

MATERIALS AND METHODS

In the siliciclastic sequence with biogenic carbonate and organic matter at Bass River, a change from glauconite-rich sandy silts to clay and the onset of the CIE at ~ 357.3 m below surface (mbs) mark the transition from the Paleocene into the PETM (Cramer et al., 1999). Well-preserved (i.e., showing no signs of degradation) dinocysts are abundant throughout the record (Sluijs and Brinkhuis, 2009).

Palynological residues of Sluijs and Brinkhuis (2009) were washed using sieving (15 μm) and ultrasonic cleaning in Milli-Q water to exclude contamination with amorphous particulate organic matter. Individual dinocysts of the species *Apectodinium homomorphum*, *Areoligera volata*, *Spiniferites ramosus* (and closely resembling specimens), and *Eocladopyxis peniculata* were pressed on a nickel sample tray, which was then placed in a miniaturized ablation chamber. In our LA-nC-GC-IRMS setup (Van Roij et al., 2017), molecular dinocyst fragments resulting from deep ultraviolet LA are transported into capillaries on a helium carrier gas, and subsequently oxidized in a combustion oven. The CO_2 formed is transported to a GC combustion interface, and subsequently into a ThermoFisher DeltaV Advantage IRMS for $\delta^{13}\text{C}$ analysis.

Analyses of the International Atomic Energy Agency CH-7 polyethylene standard (PE; certified $\delta^{13}\text{C}$ value $-32.151\text{‰} \pm 0.050\text{‰}$; 1σ) show 0.41‰ precision and 0.36‰ accuracy for analyses yielding peak areas of at least 4 voltseconds (Vs), equivalent to >42 ng C (Van Roij et al., 2017). Precision decreases at lower yields, so that multiple specimens need to be analyzed to achieve low standard errors. We therefore typically perform 20–50 analyses of individual specimens of the relatively thick-walled *A. homomorphum* and large *A. volata*. Because of their thin cyst wall, 3–5 specimens of *S. ramosus* and *E. peniculata* were analyzed simultaneously for a single measurement. Calibration to the Vienna Peedee belemnite (VPDB) scale was achieved through bracketing series of analyses by the PE standard (>4 Vs).

¹GSA Data Repository item 2018018, Figures DR1–DR3 (site location, all isotope results in histograms, and dinocyst assemblages), and Table DR1 (raw isotope data), is available online at <http://www.geosociety.org/datarepository/2018/> or on request from editing@geosociety.org.

RESULTS AND DISCUSSION

Data Quality and Variability

Individual ablations yielded between 0.1 and 3.4 Vs and produced a broad range of $\delta^{13}\text{C}$ values (Fig. DR2). At a similar signal range, PE analyses show a 1σ uncertainty of $\sim 0.5\text{‰}$ – 1.7‰ (Van Roij et al., 2017), which for most samples and species is similar to the general variability observed between the dinocysts studied here. It is unclear, however, if the PE standard is homogeneous on the micrometer scale (Van Roij et al., 2017). This result implies that the variability between specimens within most samples does not significantly exceed the analytical uncertainty. Shapiro-Wilk tests show that the distributions of the populations are (close to) normal (Fig. DR2). Moreover, small peak areas correspond to relatively high scatter, and high peak areas correspond to $\delta^{13}\text{C}$ values that are close to the mean of the populations. We recorded no sample-size dependency (Fig. DR2).

For a few samples and species, particularly Paleocene *A. volata*, the variance in dinocyst $\delta^{13}\text{C}$ significantly ($p < 0.05$) exceeds that of the standard (Fig. DR2). Part of the variance therefore relates to variability within populations. It is interesting that the variance in *A. volata* is significantly smaller than that of the standard in PETM sample at 356.84 mbs ($n = 43$), suggesting that this population is isotopically more homogeneous than the PE standard.

CIE in Dinocyst $\delta^{13}\text{C}$ Records

Normality of the data sets implies that the absolute values of the populations can be assessed by means and standard errors of the means (Fig. 1). Mean $\delta^{13}\text{C}$ values of *S. ramosus* are -24.9‰ just below the CIE. At the onset of the CIE, at 357.3 mbs, $\delta^{13}\text{C}$ values shift to a mean of -27.1‰ , implying a CIE of 2.2‰ (± 0.46 , 1 standard error, SE). Only one data point could be generated below the CIE for *A. homomorphum* and above the CIE for *A. volata* due to scarcity of these species in these intervals. The difference between the means of uppermost Paleocene and lowermost PETM samples suggest a CIE of 1.8‰ (± 0.36 , 1 SE) for *A. volata* and 4.0‰ (± 0.54 , 1 SE) for *A. homomorphum*. Regardless of these species-specific differences, the results imply that dinocyst $\delta^{13}\text{C}$ is primarily controlled by the $\delta^{13}\text{C}$ of DIC at the time of formation.

It is interesting that the CIEs in these single-species records are somewhat smaller in magnitude than that recorded in a previously published bulk dinocyst $\delta^{13}\text{C}$ record, based on an optimally sieved palynological residue that dominantly comprised dinocysts (Sluijs et al., 2007) (Fig. 1). While absolute $\delta^{13}\text{C}$ values of this record correspond well with the species-specific records in the Paleocene, bulk values are 1‰ – 2‰ more ^{13}C -depleted in the early stages of the CIE. This is unexpected, as the bulk record should reflect a weighted average of *Spiniferites* and *Apectodinium*, the dominant dinocysts within these samples. We therefore also analyzed the $\delta^{13}\text{C}$ of amorphous organic matter, using LA-nC-GC-IRMS, which was originally considered to be a negligible factor based on light microscopic observations (Sluijs et al., 2007). The amorphous organic matter, which is almost absent in the Paleocene but present in the PETM, is, however, very depleted in ^{13}C (Fig. 1), implying that even a mass contribution of 10%–20% would skew bulk dinocyst records toward recorded low values and result in a large CIE. Considering $\delta^{13}\text{C}$ constraints on Paleocene–Eocene terrestrial and marine organic matter (Hayes et al., 1999; Sluijs and Dickens, 2012), the extremely low value suggests that the amorphous matter is of marine origin.

The bulk dinocyst record was generated to demonstrate that the observed onset of the *Apectodinium* acme (Crouch et al., 2001) prior to the onset of the CIE, as measured on carbonate, was not an artifact of selective bioturbation. Here our species-specific record confirms that the abundant *Apectodinium* at 357.58 mbs (Fig. DR3) yield Paleocene $\delta^{13}\text{C}$ values and thus that the *Apectodinium* acme precedes the CIE. The magnitude of the CIE in *A. homomorphum* (4‰) is slightly larger than that recorded in the mixed-layer foraminifer *Acarinina* spp. at Bass River

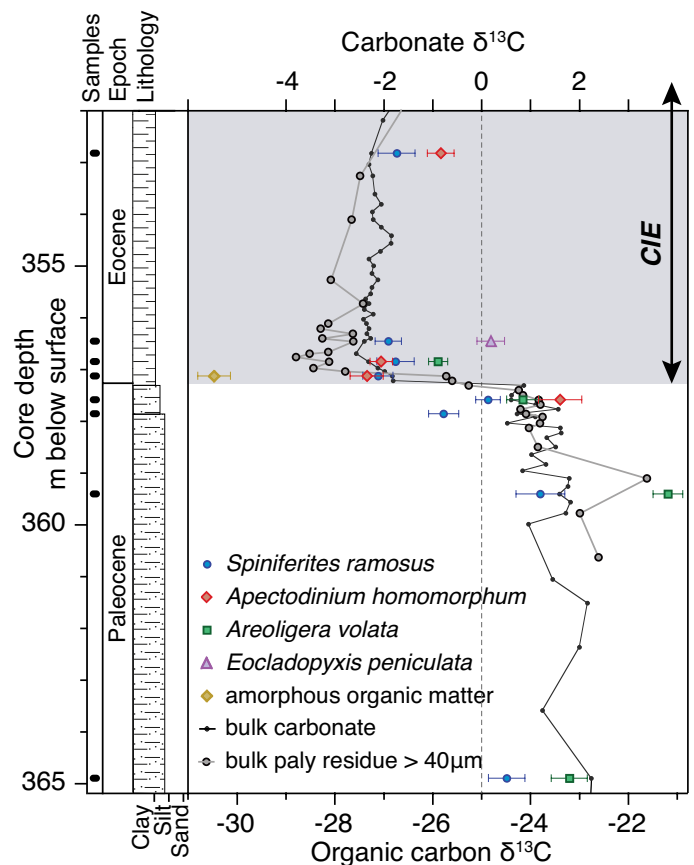


Figure 1. Dinocyst species-specific carbon isotope records from the Paleocene-Eocene Thermal Maximum (PETM) at Ocean Drilling Program Site Bass River, New Jersey, USA. The bulk carbonate record is from John et al. (2008), and the bulk palynological (paly) $>40\ \mu\text{m}$ record that dominantly comprises dinocysts is from Sluijs et al. (2007). Data points are mean values of 20–50 analyses on single specimens of *Apectodinium homomorphum* and *Areoligera volata* and 3–5 specimens of *Spiniferites ramosus* and *Eoeladopyxis peniculata*. Error bars reflect 1 standard error of the mean. The $\delta^{13}\text{C}$ scales are offset by 25‰. Values are expressed (‰) relative to the Vienna Pee Dee belemnite standard. CIE—carbon isotope excursion.

(3.4‰ ; John et al., 2008), possibly indicating an increase in ^{13}C fractionation due to the PETM rise in CO_2 (Hoins et al., 2015).

Dinocyst $\delta^{13}\text{C}$ Ecology

The records also show differences in $\delta^{13}\text{C}$ values between species, related to differences in ecology and/or biosynthesis (Fig. 1). Populations of *A. volata* are enriched in ^{13}C relative to *S. ramosus* for all 4 samples where both could be analyzed, typically by $\sim 1\text{‰}$. The PETM $\delta^{13}\text{C}$ value of *E. peniculata* is strikingly high, broadly comparable to Paleocene values of the other taxa. Just as remarkable is the changing offset between *S. ramosus* and *A. homomorphum* across the PETM: *A. homomorphum* is relatively ^{13}C enriched in the latest Paleocene and toward the top of the PETM, while the species are statistically indistinguishable in the lowermost part of the CIE. This implies that at least one of these species underwent a significant change in carbon acquisition or ecological niche across the onset of the PETM.

Differences in dinocyst species-specific $\delta^{13}\text{C}$ values could originate from several ecological factors. Dinoflagellates may be autotrophic, mixotrophic, or heterotrophic, which may affect cyst $\delta^{13}\text{C}$. Such strategies are known for many extant species and evolutionary lineages (*Spiniferites* and *Eoeladopyxis*) but not well constrained for extinct groups (*Areoligera* and *Apectodinium*). Culturing experiments on autotrophic taxa have

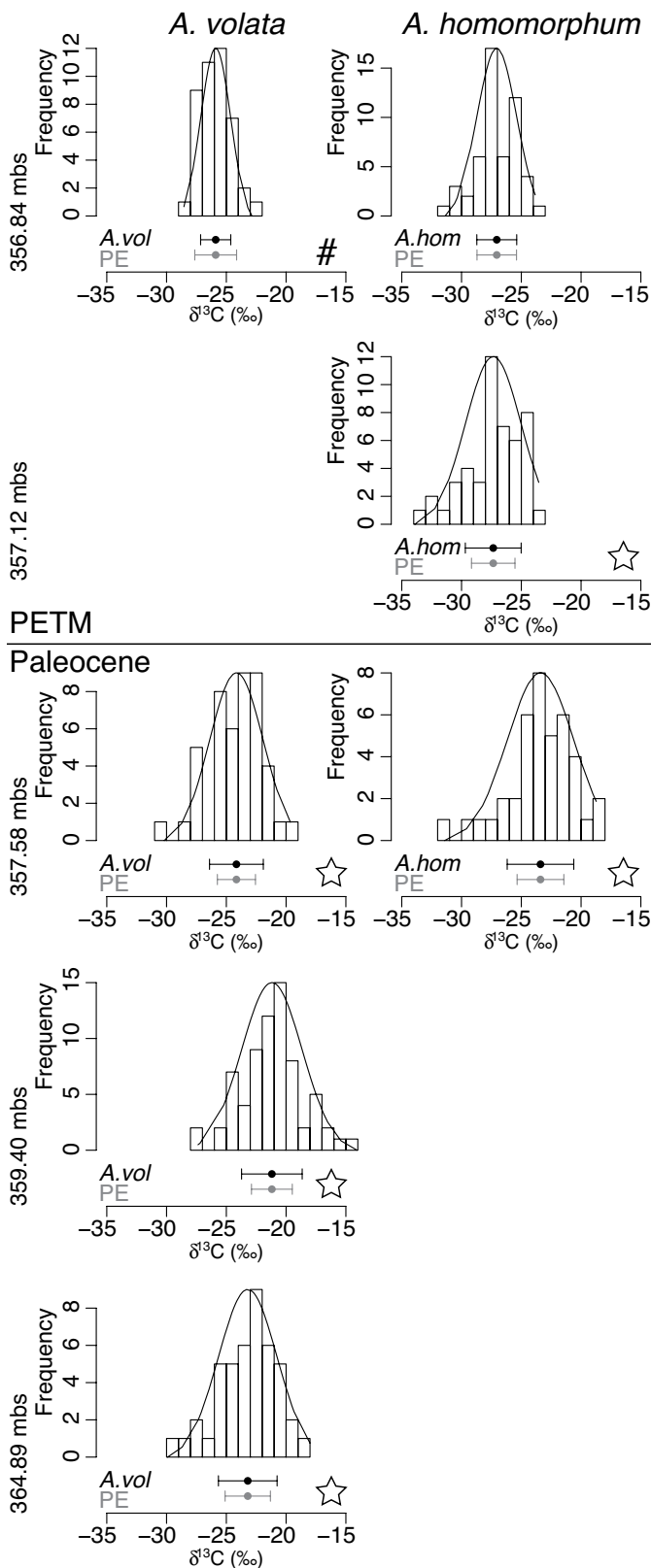


Figure 2. Frequency distribution of $\delta^{13}\text{C}$ analyses of individual *Areoligera volata* and *Apectodinium homomorphum* specimens (mbs—m below surface). Error bars reflect 1 standard error of the mean of dinocyst $\delta^{13}\text{C}$ analyses and the International Atomic Energy Agency CH-7 polyethylene (PE) standard. The variance of *A. volata* in the sample marked by # is significantly smaller than that of the PE standard, while stars indicate samples in which dinocyst $\delta^{13}\text{C}$ variance significantly exceeds that of the standard ($p < 0.05$).

shown species-specific fractionation resulting from differences in carbon acquisition (Hoins et al., 2015, 2016a, 2016b; Rost et al., 2006). Many dinoflagellates take up both dissolved CO_2 and HCO_3^- for fixation, but their relative contributions differ between species (Hoins et al., 2016b; Rost et al., 2006). Because seawater CO_2 is depleted in ^{13}C relative to HCO_3^- by 8‰–12‰ depending on temperature (Mook et al., 1974), this may contribute appreciably to differences between species. Dinoflagellate ^{13}C fractionation might also increase because of changing influx and leakage of inorganic carbon through the cell per unit of time. Increased fluxes of CO_2 result in more efficient replenishment of the intracellular stock of ^{12}C , so that the resulting fractionation of the cell is closer to the maximum of RuBisCO (ribulose-1,5-bisphosphate carboxylase/oxygenase; Hoins et al., 2016b; Sharkey and Berry, 1985). In addition, changes in seawater $\delta^{13}\text{C}_{\text{DIC}}$ related to the seasonal cycle or depth habitat may result in species-specific $\delta^{13}\text{C}$ differences. Some photosynthetic dinoflagellate species may deplete seawater from ^{12}C as they occur in massive blooms of as many as 10^7 cells/L of seawater (e.g., Heiskanen, 1993).

We consider the latter factor a likely explanation for the high $\delta^{13}\text{C}$ values of *E. peniculata*. This species is evolutionary related to modern *Pyrodinium bahamense*, which causes harmful blooms (McLean, 1976). The high $\delta^{13}\text{C}$ values are thus in line with a short, intense growing season, similar to *P. bahamense* in present oceans, which locally depleted seawater DIC from ^{12}C . This interpretation is also consistent with very high $\delta^{13}\text{C}$ values (to -18.9‰) of *Eocladopyxis*-dominated (73%; 10^5 cysts/g) palynological residues at the onset of the PETM in a Nigerian section (Frieling et al., 2017).

Recent controlled growth experiments have indicated that ^{13}C fractionation in the dinoflagellate *Gonyaulax spinifera*, which produces *S. ramosus* dinocysts, increases with higher CO_2 concentrations due to increased leakage (Hoins et al., 2015, 2016b). *S. ramosus*, however does not show a larger CIE relative to biogenic carbonate that would be expected from the increase in $p\text{CO}_2$ during the PETM (Fig. 1). Concentrations of CO_2 across the PETM were likely higher than those in the culturing experiments, so possibly maximum ^{13}C fractionation was already reached prior to the CIE. Alternatively, a shift of the dominant season of production or depth habitat might have reduced the difference between dinocyst and carbonate $\delta^{13}\text{C}$. Similar to other proxies, a CO_2 proxy based on dinocysts may thus possibly be biased during phases of massive ecological change in such marginal settings.

Added Value of Single-Specimen Isotopic Analyses

A. volata exhibits relatively high $\delta^{13}\text{C}$ values. *Areoligera* was likely autotrophic and is typically associated with relatively shallow, high-energy settings (Brinkhuis, 1994; Sluijs and Brinkhuis, 2009). With the available information, it is not possible to determine whether it occurred in seasonal blooms, used relatively high amounts of HCO_3^- during carbon acquisition, leaked little CO_2 , or fixed carbon close to the sea surface. Regardless of the absolute $\delta^{13}\text{C}$ values, *A. volata* exhibits considerable variability prior to the CIE ($1\sigma = 2.2\text{‰}$ – 2.5‰), while variability is significantly smaller in the sample within the CIE ($1\sigma = 1.26\text{‰}$; Fig. 2). This suggests that the niche of this species, geographically or in (annual) duration of presence, became limited during the CIE. This species is present in very low numbers only during the PETM at the study site (Fig. DR3), hypothesized to reflect sea-level rise (Sluijs and Brinkhuis, 2009). Comparison to the variance in carbon isotopic values in *A. homomorphum* shows that the fitness of this species is not affected across the PETM, which is in line with its acme, as *A. volata* collapsed. Crucially, this indicates that the variance in single specimen $\delta^{13}\text{C}$ populations can yield information on the ecological fit and/or fitness of species.

CONCLUSIONS

We present the first ever species-specific dinoflagellate cyst $\delta^{13}\text{C}$ records. *Apectodinium homomorphum*, *Areoligera volata*, and *Spiniferites*

ramosus all show the characteristic negative carbon isotope excursion across the PETM at Bass River, New Jersey. Differences in absolute values and the magnitude of the CIE are attributed to changes in carbon acquisition, food source, and dominant season and depth of production. The records confirm that the first anomalous *Apectodinium* abundance leads the input of ^{13}C -depleted carbon marking the CIE. It represents the first anomalous change related to the PETM. Changes in the variance in single specimen $\delta^{13}\text{C}$ populations suggest a decline in the ecological fitness of *A. volata* during the PETM, underlining the potential of this novel analytical approach to unravel the impact of environmental crises.

ACKNOWLEDGMENTS

We thank Niels Waarlo for analytical support. Sluijs thanks the European Research Council for Starting Grant 259627. This work was carried out under the program of the Netherlands Earth System Science Centre, financially supported by the Dutch Ministry of Education, Culture, and Science. We thank Erica Crouch and an anonymous reviewer for thoughtful reviews.

REFERENCES CITED

- Brinkhuis, H., 1994, Late Eocene to early Oligocene dinoflagellate cysts from the Priabonian type-area (northeast Italy); biostratigraphy and palaeoenvironmental interpretation: *Palaeogeography, Palaeoclimatology, Palaeoecology*, v. 107, p. 121–163, [https://doi.org/10.1016/0031-0182\(94\)90168-6](https://doi.org/10.1016/0031-0182(94)90168-6).
- Cramer, B.S., Aubry, M.-P., Miller, K.G., Olsson, R.K., Wright, J.D., and Kent, D.V., 1999, An exceptional chronologic, isotopic, and clay mineralogic record of the latest Paleocene thermal maximum, Bass River, NJ, ODP 174AX: *Bulletin de la Société Géologique de France*, v. 170, p. 883–897, <https://doi.org/10.7916/D8222RZR>.
- Crouch, E.M., Heilmann-Clausen, C., Brinkhuis, H., Morgans, H.E.G., Rogers, K.M., Egger, H., and Schmitz, B., 2001, Global dinoflagellate event associated with the late Paleocene thermal maximum: *Geology*, v. 29, p. 315–318, [https://doi.org/10.1130/0091-7613\(2001\)029<0315:GDEAWT>2.0.CO;2](https://doi.org/10.1130/0091-7613(2001)029<0315:GDEAWT>2.0.CO;2).
- Dickens, G.R., Castillo, M.M., and Walker, J.C.G., 1997, A blast of gas in the latest Paleocene: Simulating first-order effects of massive dissociation of oceanic methane hydrate: *Geology*, v. 25, p. 259–262, [https://doi.org/10.1130/0091-7613\(1997\)025<0259:ABOGIT>2.3.CO;2](https://doi.org/10.1130/0091-7613(1997)025<0259:ABOGIT>2.3.CO;2).
- Dunkley Jones, T., Lunt, D.J., Schmidt, D.N., Ridgwell, A., Sluijs, A., Valdes, P.J., and Maslin, M., 2013, Climate model and proxy data constraints on ocean warming across the Paleocene-Eocene Thermal Maximum: *Earth-Science Reviews*, v. 125, p. 123–145, <https://doi.org/10.1016/j.earscirev.2013.07.004>.
- Frieling, J., Gebhardt, H., Huber, M., Adekeye, O.A., Akande, S.O., Reichart, G.-J., Middelburg, J.J., Schouten, S., and Sluijs, A., 2017, Extreme warmth and heat-stressed plankton in the tropics during the Paleocene-Eocene Thermal Maximum: *Science Advances*, v. 3, e1600891, <https://doi.org/10.1126/sciadv.1600891>.
- Gibbs, S.J., Bown, P.R., Murphy, B.H., Sluijs, A., Edgar, K.M., Päläike, H., Bolton, C.T., and Zachos, J.C., 2012, Scaled biotic disruption during early Eocene global warming events: *Biogeosciences*, v. 9, p. 4679–4688, <https://doi.org/10.5194/bg-9-4679-2012>.
- Hayes, J.M., Strauss, H., and Kaufmann, A.J., 1999, The abundance of ^{13}C in marine organic matter and isotopic fractionation in the global biogeochemical cycle of carbon during the past 800 Ma: *Chemical Geology*, v. 161, p. 103–125, [https://doi.org/10.1016/S0009-2541\(99\)00083-2](https://doi.org/10.1016/S0009-2541(99)00083-2).
- Heiskanen, A.-S., 1993, Mass encystment and sinking of dinoflagellates during a spring bloom: *Marine Biology*, v. 116, p. 161–167, <https://doi.org/10.1007/BF00350743>.
- Hoins, M., Eberlein, T., Großmann, C., Brandenburg, K., Reichart, G.-J., Rost, B., Sluijs, A., and Van de Waal, D.B., 2016a, Combined effects of ocean acidification and light or nitrogen availabilities on ^{13}C fractionation in marine dinoflagellates: *PLoS One*, v. 11, e0154370, <https://doi.org/10.1371/journal.pone.0154370>.
- Hoins, M., Eberlein, T., Van de Waal, D.B., Sluijs, A., Reichart, G.-J., and Rost, B., 2016b, CO_2 -dependent carbon isotope fractionation in dinoflagellates relates to their inorganic carbon fluxes: *Journal of Experimental Marine Biology and Ecology*, v. 481, p. 9–14, <https://doi.org/10.1016/j.jembe.2016.04.001>.
- Hoins, M., Van de Waal, D.B., Eberlein, T., Reichart, G.-J., Rost, B., and Sluijs, A., 2015, Stable carbon isotope fractionation of organic cyst-forming dinoflagellates: Evaluating the potential for a CO_2 proxy: *Geochimica et Cosmochimica Acta*, v. 160, p. 267–276, <https://doi.org/10.1016/j.gca.2015.04.001>.
- John, C.M., Bohaty, S.M., Zachos, J.C., Sluijs, A., Gibbs, S.J., Brinkhuis, H., and Bralower, T.J., 2008, North American continental margin records of the Paleocene-Eocene thermal maximum: Implications for global carbon and hydrological cycling: *Paleoceanography*, v. 23, PA2217, <https://doi.org/10.1029/2007PA001465>.
- Kopp, R.E., Schumann, D., Raub, T.D., Powars, D.S., Godfrey, L.V., Swanson-Hysell, N.L., Maloof, A.C., and Vali, H., 2009, An Appalachian Amazon? Magnetofossil evidence for the development of a tropical river-like system in the mid-Atlantic United States during the Paleocene-Eocene thermal maximum: *Paleoceanography*, v. 24, PA4211, <https://doi.org/10.1029/2009PA001783>.
- Matthiessen, J., DeVernal, A., Head, M., Okolodkov, Y., Zonneveld, K., and Harland, R., 2005, Recent and Quaternary organic-walled dinoflagellate cysts in arctic marine environments and their paleoenvironmental significance: *Paläontologische Zeitschrift*, v. 79, p. 3–51, <https://doi.org/10.1007/BF03021752>.
- McLean, D.M., 1976, *Eocladopyxis peniculatum* Morgenroth, 1966, Early Tertiary ancestor of the modern dinoflagellate *Pyrodinium bahamense* Plate, 1906: *Micropaleontology*, v. 22, p. 347–351, <https://doi.org/10.2307/1485256>.
- Mook, W.G., Bommerson, J.C., and Staverman, W.H., 1974, Carbon isotope fractionation between dissolved bicarbonate and gaseous carbon dioxide: *Earth and Planetary Science Letters*, v. 22, p. 169–176, [https://doi.org/10.1016/0012-821X\(74\)90078-8](https://doi.org/10.1016/0012-821X(74)90078-8).
- Rost, B., Richter, K.-U., Riebesell, U., and Hansen, P.J., 2006, Inorganic carbon acquisition in red tide dinoflagellates: *Plant, Cell & Environment*, v. 29, p. 810–822, <https://doi.org/10.1111/j.1365-3040.2005.01450.x>.
- Sharkey, T.D., and Berry, J.A., 1985, Carbon isotope fractionation of algae as influenced by an inducible CO_2 concentrating mechanism, *in* Lucas, W.J., and Berry, J.A., eds., *Inorganic carbon uptake by aquatic photosynthetic organisms*: Rockville, Maryland, American Society of Plant Physiologists, p. 389–401.
- Sluijs, A., and Brinkhuis, H., 2009, A dynamic climate and ecosystem state during the Paleocene-Eocene Thermal Maximum: Inferences from dinoflagellate cyst assemblages on the New Jersey Shelf: *Biogeosciences*, v. 6, p. 1755–1781, <https://doi.org/10.5194/bg-6-1755-2009>.
- Sluijs, A., and Dickens, G.R., 2012, Assessing offsets between the $\delta^{13}\text{C}$ of sedimentary components and the global exogenic carbon pool across early Paleogene carbon cycle perturbations: *Global Biogeochemical Cycles*, v. 26, GB4005, <https://doi.org/10.1029/2011GB004224>.
- Sluijs, A., Pross, J., and Brinkhuis, H., 2005, From greenhouse to icehouse; organic-walled dinoflagellate cysts as paleoenvironmental indicators in the Paleogene: *Earth-Science Reviews*, v. 68, p. 281–315, <https://doi.org/10.1016/j.earscirev.2004.06.001>.
- Sluijs, A., Brinkhuis, H., Schouten, S., Bohaty, S.M., John, C.M., Zachos, J.C., Reichart, G.-J., Sinninghe Damsté, J.S., Crouch, E.M., and Dickens, G.R., 2007, Environmental precursors to light carbon input at the Paleocene/Eocene boundary: *Nature*, v. 450, p. 1218–1221, <https://doi.org/10.1038/nature06400>.
- Van de Waal, D.B., John, U., Ziveri, P., Reichart, G.J., Hoins, M., Sluijs, A., and Rost, B., 2013, Ocean acidification reduces growth and calcification in a marine dinoflagellate: *PLoS One*, v. 8, e65987, <https://doi.org/10.1371/journal.pone.0065987>.
- Van Rooij, L., Sluijs, A., Laks, J.J., and Reichart, G.-J., 2017, Stable carbon isotope analyses of ng quantities of particulate organic carbon (pollen) with laser ablation nano combustion gas chromatography isotope ratio mass spectrometry: *Rapid Communications in Mass Spectrometry*, v. 31, p. 47–58, <https://doi.org/10.1002/rcm.7769>.
- Zachos, J.C., et al., 2005, Rapid acidification of the ocean during the Paleocene-Eocene Thermal Maximum: *Science*, v. 308, p. 1611–1615, <https://doi.org/10.1126/science.1109004>.

Manuscript received 7 August 2017

Revised manuscript received 20 October 2017

Manuscript accepted 25 October 2017

Printed in USA